International Symposium on Lowland Technology (ISLT 2018)
Sept. 26 – 28, 2018, Hanoi, Vietnam. ÍSBN: 978.604.82.2483.7

NUMERICAL MODELLING OF FLOW IN THE TONLE SAP BY MEANS OF A DISCONTINUOUS GALERKIN FINITE-ELEMENT MODEL

Hoang-Anh Le [1,2], Chien Pham Van [3], Huyen Xuan Vu Dang[4], Jonathan Lambrechts[5], Sigrun Ortleb[6], Nicolas Gratiot[7], Sandra Soares-Frazao[8] and Eric Deleersnijder[9,10]

[1] Civil and Environmental Engineering, Institute of Mechanics, Materials and Civil Engineering (IMMC), Université catholique de Louvain, Place du Levant 1, B-1348 Louvain – la – Neuve, email: anh.le@uclouvain.be, Belgium
[2] Asian Research Center on Water (CARE-Rescif), Ho Chi Minh City University of Technology, Block B7, 268 Ly Thuong Kiet Street, District 10, Ho Chi Minh City, email: anh.le@uclouvain.be, Vietnam
[3] Thuyloi University, 175 Tay Son, Hanoi, Vietnam; email:Pchientvct_tv@tlu.edu.vn
[4] Asian Research Center on Water (CARE-Rescif), Ho Chi Minh City University of Technology, Block B7, 268 Ly Thuong Kiet Street, District 10, Ho Chi Minh City, email: xhuyen@yahoo.com, Vietnam
[5] Université catholique de Louvain, Institute of Mechanics, Materials and Civil Engineering (IMMC), 4 avenue Georges Lemaître, B-1348 Louvain – la – Neuve, email: jonathan.lambrechts@uclouvain.be, Belgium
[6] Universität Kassel, FB 10, Institut für Mathematik, Heinrich-Plett-Straße 40, D-34132 Kassel, email: ortleb@mathematik.uni-kassel.de, Germany
[7] Asian Research Center on Water (CARE-Rescif), Ho Chi Minh City University of Technology, Block B7, 268 Ly Thuong Kiet Street, District 10, Ho Chi Minh City, email: nicolas.gratiot@ird.fr, Vietnam
[8] Civil and Environmental Engineering, Institute of Mechanics, Materials and Civil Engineering (IMMC), Université catholique de Louvain, Place du Levant 1, B-1348 Louvain – la – Neuve, email: sandra.soares-frazao@uclouvain.be, Belgium
[9] Université catholique de Louvain, Institute of Mechanics, Materials and Civil Engineering (IMMC), 4 avenue Georges Lemaître, B-1348 Louvain – la – Neuve, email: eric.deleersnijder@uclouvain.be, Belgium
[10] Delft University of Technology, Delft Institute of Applied Mathematics (DIAM), Van Mourik Broekmanweg 6, 2628XE Delft, The Netherlands

ABSTRACT: The Tonle Sap Lake, which is located in the Cambodian floodplain of the Mekong River System, plays an important role for storage and water supply in Cambodia as well as in the low land region of the Mekong River System. Every year the lake stores water in the flood season from May to October while it acts as a spillway providing water to the Mekong Delta in the dry season from November to April. In other words, the lake depth can rise by approximately 10 m and the water volume can increase 5 times during the year, showing various drying and wetting areas in the lake and its adjacent floodplains. In terms of hydrodynamic modelling, these wetting/drying areas are still challenging because of several difficulties, e.g. large CPU time, slow transition of wet-dry interface and, possibly lack of mass conservation. In this paper, we present a wetting - drying algorithm with a limitation for the fluid depth and a blending parameter in order to ensure local mass conservation and rapid transition of a wet/dry interface. The technique is firstly implemented in the framework of the Second-generation Louvain-la-Neuve Ice-ocean Model (SLIM). Then, it is validated by means of the analytical Balzano 1, Balzano 3 and Thacker test cases, showing its well-balancing property. Finally, it is applied to the simulation of the flow in the Tonle Sap and its neighborhood.

Keywords: Mekong, Tonle Sap, Wetting – drying algorithm, SLIM.

INTRODUCTION

Wetting – drying is an important process in environmental water flows for both physical and biological reasons, especially during extreme events (Warner et al., 2013). Thus the accurate simulation of overland flooding and drying in river floodplains and coastal zones over the world is still an outstanding challenge for hydrodynamic modelers, even though the development of powerful and accessible computers offer considerable opportunities to solve accurately the shallow water equations (e.g. D'Alpaos & Defina, 2007). Dealing with very shallow flows, temporary submergences, a wide spectrum of time scales and complex morphologies often requires very high spatial and temporal resolutions (Medeiros et al., 2013). This issue has received considerable attention in recent three decades. The solutions may be the adaptation of numerical grid at each time step to follow the deforming flow domain or retaining a fixed computational grid together with utilizing an additional wetting-drying algorithm (D'Alpaos & Defina, 2007). The implementation of a moving mesh approach is difficult, especially in a complicated bathymetry and flow configuration (Vater et al., 2015). For the second type of approaches, various formulations were developed and integrated in numerical programs. All algorithms must ensure both local and global mass conservation together with momentum conservation (Dresback et al., 2002). Each scheme has strengths and weaknesses. According to Medeiros et al., (2013), there are three categories of wetting - drying algorithms:

(1) Thin film and element removal algorithm: a threshold depth is imposed in the whole computational domain. If the water depth is lower than this threshold, this element is considered dry and the velocity is set to zero, this element will be removed from the computation mesh. This threshold however corresponds to substantial water volume in the dry areas (Casulli, 2008). The biggest problem of this algorithm is a rapid transfer of elements from dry to wet states near the wetting front. The solution requires higher mesh spatial resolution and smaller time steps.So the computational cost is usually high, and mass and momentum are not conserved.

(2) Depth extrapolation algorithms: the depth in the dry cell is extrapolated from the surrounding wet cells. Dry elements are wetted artificially. Mass conservation is affected and, hence, needs to be enforced by correction schemes.

(3) Negative depth algorithms: the model can run with negative depths, subsurface flow being controlled by porosity terms. However, the major disadvantages of this approach are that artificial porosity is applied not only to negative depths but also to a certain height above the actual sea or riverbed (Martin et al., 2018).

In the present paper, the algorithm developed by Vater et al. (2015) is implemented in our discontinuous finite – element Galerkin model and tested against several test cases and in a natural domain.

The objectives of this study are (1) the implementation of a new wetting – drying algorithm in a discontinuous Galerkin finite element model; (2) the application of the new wetting – drying algorithm to reproduce the flow in the Tonle Sap, an integrated part of the Mekong system. Accordingly, this paper is organized as follows: the implicit Wetting – Drying algorithm implemented in a discontinuous finite – element Galerkin model is presented; then the application to the Tonle Sap for an extreme flooding season is achieved, after validation by means of several critical test cases. Finally, concluding remarks are presented.

WETTING – DRYING SCHEME

The finite element model SLIM

The Second-generation Louvain-la-Neuve Ice-ocean Model (SLIM, www.climate.be/slim) is a hydrodynamic model based on unstructured grid discontinuous Galerkin finite element method that has been developed at the Université catholique de Louvain, Belgium for more than ten years. SLIM includes different options, ranging from one- to three-dimensional modules: the one-dimensional version is a section-averaged model for river networks; the two-dimensional depth-averaged version is generally applied to complex domains; the three-dimensional version is a baroclinic model for coastal flows that solves the 3D hydrostatic equations under the Boussinesq approximation. The model has been applied to various domains such as the Lake Tanganyika, Africa (Gourgue et al., 2007), the Great Barrier Reef, Australia (Lambrechts et al., 2010), the Scheldt estuary in Belgium and Netherland (de Brye et al., 2010; Gourgue et al., 2013), the Mahakam Delta in Indonesia (de Brye et al., 2011; Pham Van et al., 2016), the Columbia River (Vallaeys et al., 2018), and a lake on Titan, Saturn's moon (Vincent et al., 2016), to study flow dynamics, sediment transport, water renewal timescales and ecological issues.

Governing equations

The shallow-water equations are derived by integrating over the water column the Navier–Stokes equations, assuming that the pressure is hydrostatic and the fluid density is constant. Shallow water flows are generally well represented by those equations if the water column is well mixed and the vertical dimension is much smaller than the typical horizontal scale. The conservative shallow water equations read:

$$\frac{\partial H}{\partial t} + \nabla(H\mathbf{u}) = 0 \qquad (1)$$

$$\frac{\partial H\mathbf{u}}{\partial t} + \nabla.\frac{H\mathbf{u}H\mathbf{u}}{H} + g\nabla\frac{|H|H}{2} + \frac{ng}{H^{\frac{7}{3}}}|H\mathbf{u}|H\mathbf{u} + fe_z \times H\mathbf{u} - \nabla(H\nu\nabla\mathbf{u}) = gH\nabla h \qquad (2)$$

where t is time and $\boldsymbol{\nabla}$ is the horizontal gradient operator; H is the actual water depth, and $\mathbf{u}$ is the horizontal velocity vector averaged over the water column; H and $\mathbf{u}$ are the state variables that depend on time and position; η is free surface water above a reference level $\eta = H - h$, where h is the reference height of the water column; fe_z is the Coriolis force by z direction, n is Manning coefficient; g is the gravitational acceleration g = 9.81 m/s^2; ν is the horizontal eddy viscosity. The horizontal viscosity ν is parameterized after Smagorinsky (1963). The bed shear stress is parameterized by the Chezy - Manning - Strickler formulation.

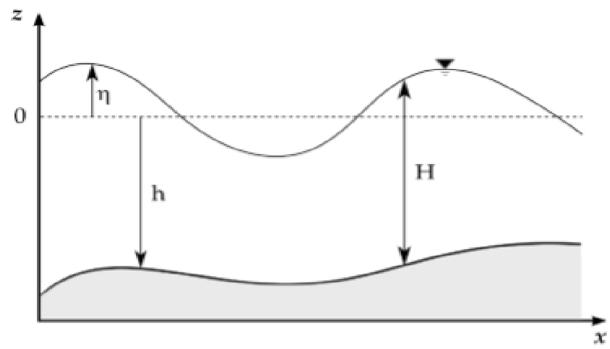

Fig. 1 Illustration of the free surface elevation η, reference depth h and actual water depth H (Pham Van, 2014)

For solving the shallow water equations, explicit time marching schemes must meet the CFL condition to ensure numerical stability, leading to small values of the time step. Implicit time marching allow for much longer time steps, which is appropriate for meshes with variable resolution and long simulations, and corresponds to choice made for the present simulations. However, to maintain this implicit time stepping even at wetting-drying fronts, appropriate algorithms have to be developed, as presented hereafter.

Wetting – Drying algorithm

This algorithm aims at solving three main problems occurring when the water depth becomes zero (H = 0): (1) the occurrence of artificial gradients in the surface elevation that can influence the momentum equation and result in an unbalanced scheme; (2) the fluid depth must remain positive; (3) ill-conditions appear when the fluid depth and momentum go to zero in case of computation of the velocity $\mathbf{u} = (H\mathbf{u}) / H$.

The idea of the proposed algorithm (Vater et al., 2013) is to compare the surface elevation, which is defined by f = max (H) – max (h) in each cell with a threshold value ε specified by the model users and adapted to the application. For f under this value of ε, the cell is considered dry. In partially dry cells, a flux term is considered, which includes the gravitational part and is computed based on the fluid depth from the semi-dry cell at the wet interface. This procedure may cause different, unbalanced in-cell distributions of H or η, thus an alternative limiting procedure is introduced. Since both results from either limiting in H or η are linear and should preserve the mean state, a blending parameter α is defined according to Eq. (3). It varies between 0 and 1 for minimum in-cell surface elevations Hmin and maximum in-cell bathymetry values hmin and hmax. If the value of α is 1, it means that the cell is wet, otherwise the cell í condensed to be dry. It is given by

$$\alpha = \min(1, \max(0, \frac{f - \varepsilon}{4\varepsilon})) \quad (3)$$

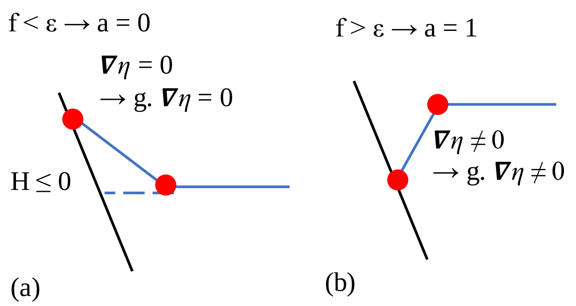

Fig. 2 Evolution of free surface by a blending parameter: (a) f value is less than the tolerant number and (b) f value is higher than the tolerant number; bathymetry (black line), water surface (blue line), water surface in dry cell (dash line) and cell nodes (dots)

Validation of the algorithm

In this section, the performances of the proposed algorithm are assessed by different test cases with analytical solutions. All test cases are in the standard SI system with m (meter), s (seconds) etc. as basic units. The discrete initial conditions and the bottom topography are derived from the analytical ones by interpolation at the nodal (cell interface) points. In the following simulations, a fixed time step is always chosen to satisfy this stability constraint.

The Balzano 1 test case

Three idealized one-dimensional test cases developed by Balzano (1998) are widely used to evaluate the accuracy of various wetting – drying methods (Yuan et al., 2008). Initially, the computational domains of these three Balzano test cases are one-dimensional basins with length of 13,800 m. However, as the purpose of this paper is to test the implementation of the new wetting - drying algorithm in the two-dimensional version of SLIM, these domains are modified by adding a width of 7,200 m. It is thus verified that the solutions of the two-dimensional simulations correspond to the one-dimensional solutions of the original Balzano test cases.

In all Balzano test cases, the Coriolis force, the surface stress and the horizontal viscosity are not taken into account. The threshold thickness ε is fixed to 0.01 m, and the simulation time step is 1 s. The only difference between the three test cases is the bathymetry.

The simulation of the 1st Balzano test case aims to simulate a wave run up on a basin with a uniform bed slope (Fig. 3). The analytical expression of the bathymetry is $h = x/2760$ where x is the coordinate in the main direction of the basin.

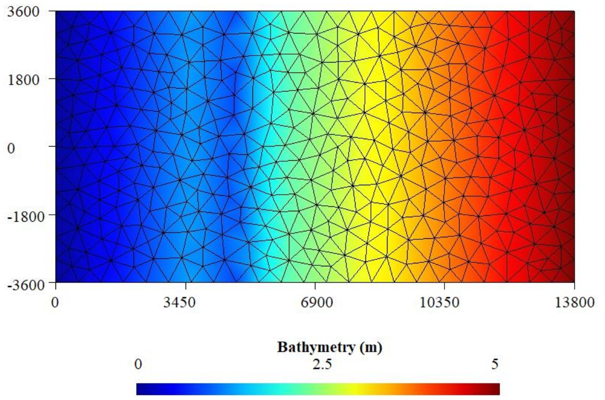

Fig. 3 Mesh generation for the Balzano 1 test case with 716 triangulars and a uniform mesh size of 500 m

A sinusoidal water level variation is imposed at the open boundary during a period of 12 h and with an amplitude of 2 m. The water depth at the open boundary oscillates between -2 and 2 m. Our model shows consistent results which are in agreement with previous publications such as Gourgue et al. (2009), Karna et al. (2011) and Nielsen et al. (2003). According to the summary by Balzano (1998), some schemes cause unintended problems, for examples: wiggles in the free surface profile during the wetting phase and in the drying phase, and pronounced underestimation (negative water thickness) or overestimation (positive water thickness) in the retention volume. By applying the proposed algorithm in SLIM, the water thickness remains always positive and the retention volume is never underestimated. With the threshold value ε, the water thickness in dry areas is limited and the overestimation is controlled to very small values.

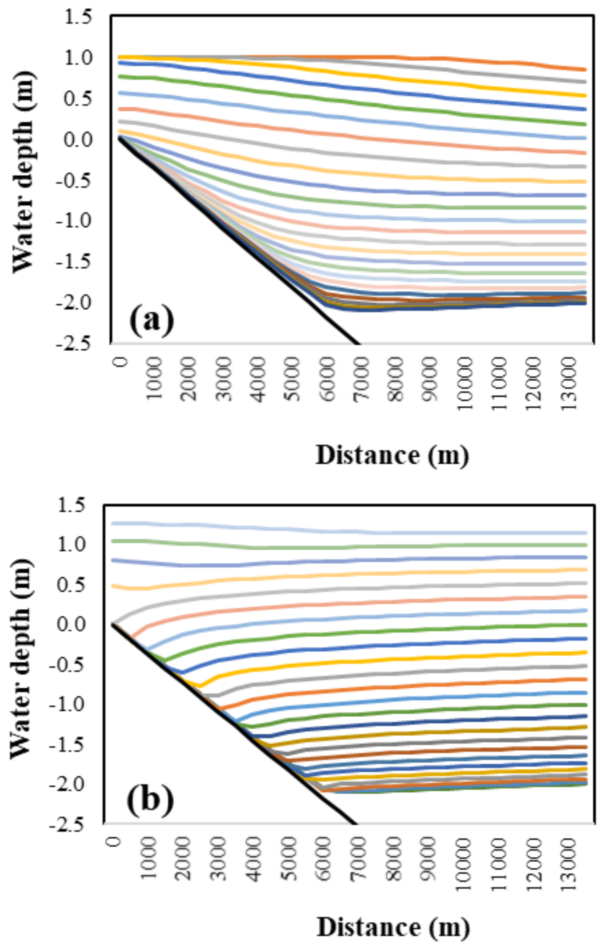

Fig. 4 Vertical section through the domain of interest, showing the bathymetry (black line) and the water surface evolution in every 600 s (colour lines), during the drying (a) and the wetting (b) phases

The Balzano 3 test case

The same simulation as the Balzano 1 test case is repeated but with a modified bathymetry. The new bathymetry contains a small reservoir that can retain water in the drying phase (Fig. 6). The analytical expression of the bathymetry is as shown below:

$h = x/2760$ if $x \leq 3600$ m or $x \geq 6000$ m

$h = 30/23$ if 3600 m $\leq x \leq 4800$ m

$h = x/1380 - 50/23$ if 4800 m $\leq x \leq 6000$ m

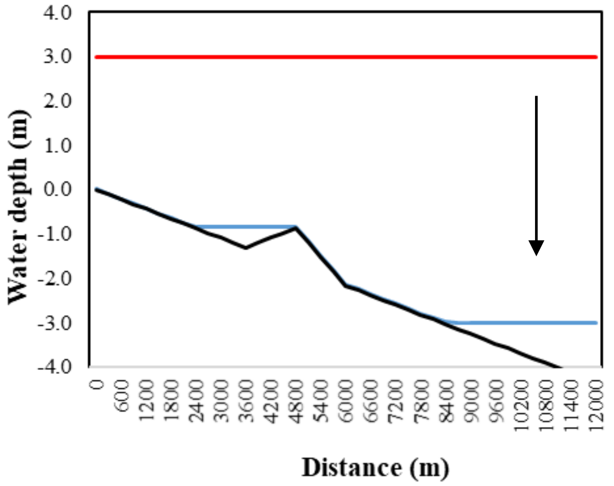

Fig. 5 Vertical section through the domain of interest, showing the bathymetry (black line) and the water surface evolution at the initial condition (red line) and equilibrium (blue line)

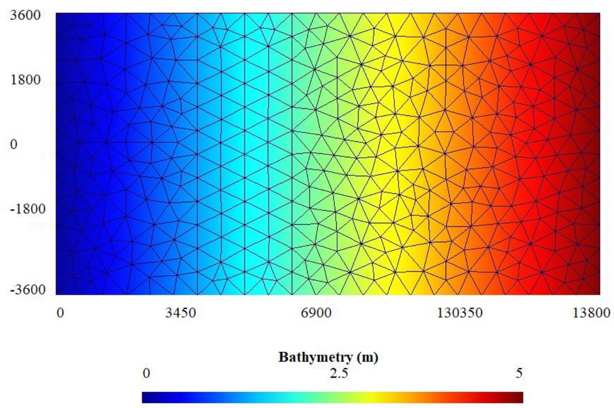

Fig. 6 Mesh used for the Balzano 3 test case with 706 triangular elements and an uniform mesh size of 600 m

A sinusoidal water level variation is imposed at the open boundary with an amplitude of 3 m initially. The water depth at the open boundary decreases from 3 to -3 m at the open boundary after 12 h of simulation. Afterwards, the water level at the open boundary is kept to -3 m. This water level is kept for an indefinitely long time in order to test whether water is leaking through the dry area, out of the small intermediate basin. Indeed, with some wetting-drying methods, some water can flow from the reservoir to the rest of the basin, even when the mean surface level inside the reservoir is below the local peak of the bathymetry. Here, after 36 h of simulation, the expected water level is reproduced in the reservoir. The physics does not seem to be altered at the limits between wet and dry areas. The simulation ends after 48 h and confirms that no negative water thickness appears in the whole domain.

The Thacker test case

This last test case, shown in Fig. 7, has also been used by Balzano (1998) to compare the best methods of its review, and also by Gourgue et al. (2009), Karna et al. (2011) and Kesserwanni et al. (2012). It is used to illustrate that a method is strictly mass conserving. This test case evaluates the inundation by the two-dimensional effects of a varying topography. The domain is a circular closed basin with radius R = 430.62 km, so that no water can enter or leave the domain; the bed is a paraboloid of revolution. At the initial time, the free surface is also a paraboloid of revolution.

Then, the free surface moves with periodical oscillations and wetting - drying occurs on the external boundary of the domain. If there is no Coriolis force, no surface stress and no dissipation (neither viscosity nor bottom stress), the analytical solution for non-linear shallow water equation is known (Thacker, 1981) so it becomes another critical test case for inundation modeling and has therefore been applied to several schemes (Vater et al., 2015). Here, the simulation mesh is generated with a gradual size of 10 m near the boundary and 100 m in the center to minimize the occurrence of wiggles. The total number of triangles is 2412. The modelling time is 48 hours, corresponding to 4 periods, to have an overview of water surface evolution in the basin.

The threshold thickness ε is fixed to 0.01 m and the simulation time step is 1 s. The analytical expressions of the bathymetry and the solution of the non-dissipative problem are shown below.

$$h = h_0 \frac{R^2 - r^2}{R^2} \tag{4}$$

$$\eta = h_0 \left(\frac{\sqrt{1-A^2}}{1 - A\cos\varpi t} - 1 - \frac{r^2}{R^2}\left(\frac{1-A^2}{(1-A\cos\varpi t)^2} - 1 \right) \right) \tag{5}$$

$$\varpi^2 = \frac{8 g h_0}{R^2} \tag{6}$$

$$A = \frac{(h_0+\eta_0)^2 - h_0^2}{(h_0+\eta_0)^2 + h_0^2} \tag{7}$$

h_0 = 50 m

η_0 = 2 m

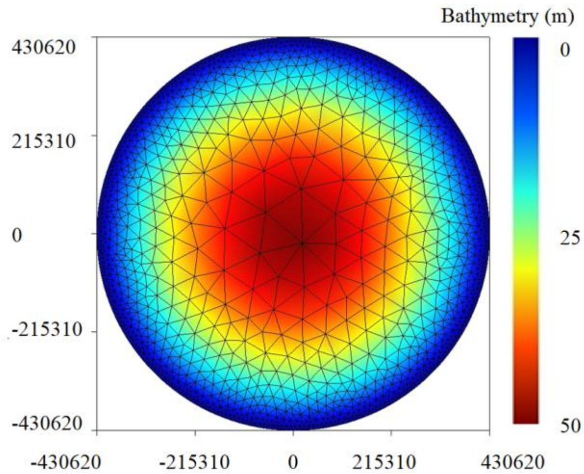

Fig. 7 Mesh generation for the Thacker test case with 2412 triangles, mesh size of 10 - 100 m and bathymetry

However, this wetting–drying method requires some dissipation to be stable, which can be observed in Fig. 8 showing the time evolution of the water level at the centre of the basin: a fairly good agreement of the results calculated by the analytical solution and the numerical solution is obtained. Several simulations have been also run with various values of the Manning coefficient n, as presented in the Fig. 9. The results with Manning coefficients appear to present more small scale oscillations of the water level than without bottom friction. The evolutions of the free surface in the center of the domain during 288 hours are shown in Fig. 10. It is clearly seen that, as expected, the water level tends to reduce and the time lag increases with higher Manning coefficients because of energy loss during its evolution.

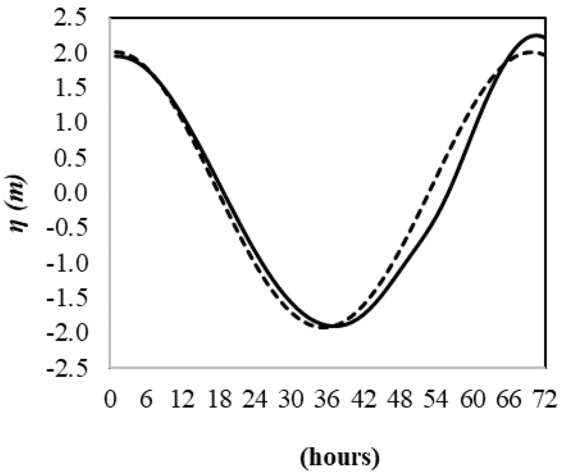

Fig. 8 Comparison of water surface elevation in the domain center by the analytical solution (dash line) and the numerical solution (continuous line)

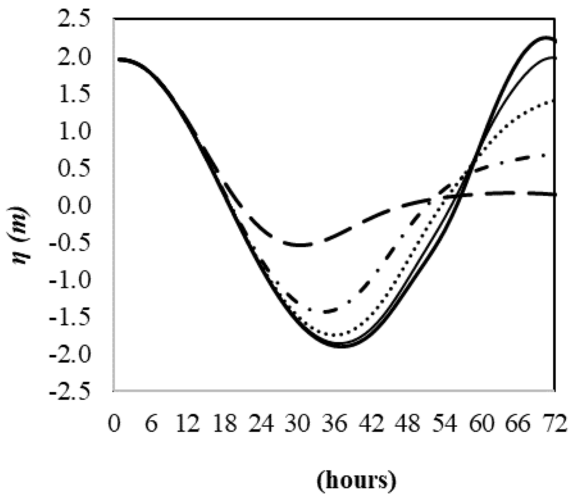

Fig. 9 Evolution of water surface elevation in the domain center with different Manning coefficients: thick line (n = 0) is the exact solution of Thacker, assuming zero dissipation; thin line (n = 0.005), dotted line (n = 0.01), dash – dotted line (n = 0.02) and dash line (n = 0.05)

Remarks on the algorithm

This wetting - drying algorithm has been well integrated in SLIM, a discontinuous Galerkin discretization of the two-dimensional shallow water equations. It is validated by several critical test cases with a variety of flow regimes; showing that the scheme is well-balanced, mass conservative and stable for rapid transitions of the wetting/drying interface. Thus optimistically this proposed technique is able to work well in a realistic and complex water body, namely in order to simulate the inundation process and subsequent drying in the Tonle Sap lake, Cambodia floodplain.

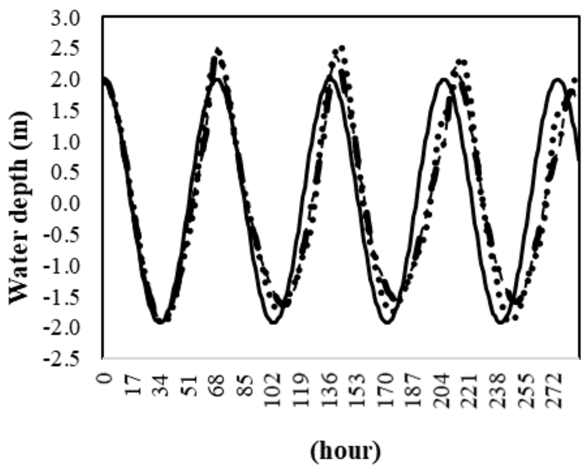

Fig. 10 Evolution of water surface elevation in the domain center with different time step: thick line (n = 0) is the exact solution of Thacker, assuming zero dissipation; dotted line (dt = 1 s), dash – dotted line (dt = 10 s) and dash line (dt = 100 s)

APPLICATION TO THE TONLE SAP

Study area

Tonle Sap is an important water body, located in the Cambodian floodplain (Kummu et al., 2014) which contributes largely to the Mekong river dynamics. It comprises a permanent lake, 12 tributaries, extensive floodplains and the Tonle Sap River. The permanent lake consists of a large part in the Northwest with dimensions of 75 km x 32 km and a small part in the Southeast with dimensions of 35 km x 28 km (Ji et al., 2018), which are connected by a narrow strait (Camphell et al., 2009). The lake and its floodplains form the largest freshwater sources in the Southeast Asia (Kummu et al., 2014). The Tonle Sap River with a length of approximately 120 km (Siev et al., 2016) is situated at the Southeast end of the Tonle Sap lake and joins the Mekong River at Chaktomuk confluence. At the confluence, the river splits into the Bassac River in the West and the Mekong River in the East.

The hydrology of the Tonle Sap is driven by the monsoonal flood regime of the whole Mekong River Basin (Penny, 2006 and Berg et al., 2007). As a result, the Tonle Sap has a unique hydrological regime. In the flooding season (from June to October), when the water level of the Mekong River is higher than in the Tonle Sap lake, reserve flows occurs from the Mekong River into the lake. In addition, discharges from the 12 tributaries and overland flow provide additional water sources for the lake. Therefore, the water level in the lake increases from 1.44 m to 9.09 m (Kummu et al., 2014). At the beginning of the dry season (November), the water level in the Tonle Sap lake reaches a peak value and its level becomes higher than the level in the Mekong River. Thus the flow starts changing its direction, from the Tonle Sap lake towards the Mekong River. Hydrologically, the lake functions as a regulatory reservoir for the Mekong Delta of Vietnam (Camphell et al., 2009 and Thanh et al., 2017), storing approximately 50 % of total Mekong inflow and releasing 90 % of outflow to the Mekong River (Royal Haskoning HDV et al., 2009), providing a freshwater inflow to the downstream in dry season (Hai et al., 2008). With this phenomenon, the catchment size varies from 7,190 to 12,720 km^2 (Kummu et al., 2014) and causes the occurrence of dry areas after water recedes.

The new wetting – drying algorithm integrated in SLIM is used to simulate this complex flow regime in the Tonle Sap. The computational domain extends over the floodplains, and is limited to the south at Prek Kdam, 35 km upstream of Phnom Phenh and at the confluence with the Mekong River at Chaktomuk. The model uses a spherical coordinate system and the multi-scale mesh is generated by the GMSH software (http://www.geuz.org/gmsh, Geuzaine & Remacle, 2009 and Lambrechts et al., 2008). The mesh consists of 246,428 elements with 122,593 nodes. The finer mesh elements are used to represent the 12 tributaries and the Tonle Sap River while the coarser mesh elements are used for the floodplains and the permanent lake. The mesh resolution varies from 100 m - 2000 m in order to take into account several physical processes occurring in the simulation domain. The application of this multi-scale mesh allows to simulate both small-scale and large-scale processes within a single model with neither nudging nor nesting (Vallaeys et al., 2018).

The bathymetry of the simulation domain was constructed from various data sets: (1) the topographical data from the Mekong River Commission (MRC, 2003) with 50 x 50 m grid resolution Digital Elevation Map (DEM); and (2) local cross-section measurement data done by Mekong River Commission to describe the bed elevation in the lake and the river. The bathymetry of the simulation topography shows variations from – 50 to 10 m (see Fig. 11).

The daily discharge from the 12 tributaries and the daily water level at Prek Kdam (downstream boundary) are imposed at the boundaries of the computational domain (Fig. 12). These data (Fig. 13) were obtained from the sources of the Mekong River Commission. No-slip and impermeability conditions are set along the close boundaries. Open boundary condition is water level variation generated from data measured at Prek Kdam.

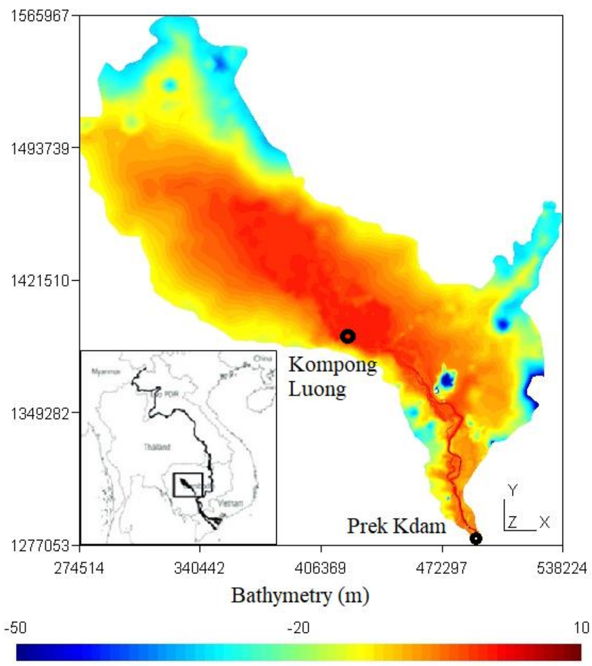

Fig. 11 Location and bathymetry of the domain with Kompong Luong station and Prek Kdam station

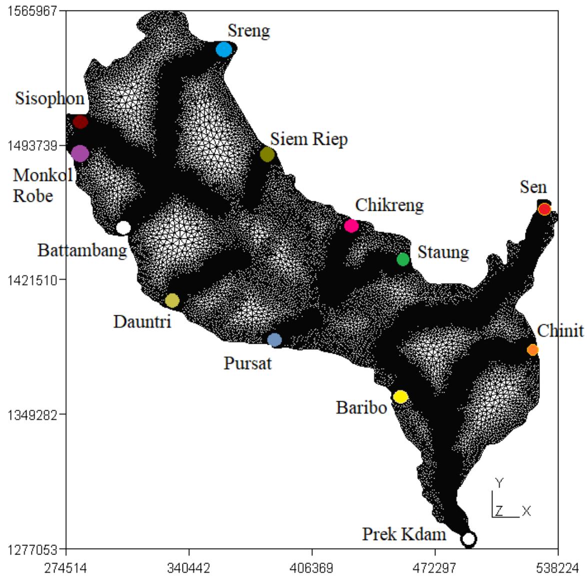

Fig. 12 Computation mesh of the domain. The color dots show the 12 stations corresponding to the tributaries as input data sources and the white dot represents for Prek Kdam station as downstream boundary of the model

The numerical simulation are performed to determine (1) the spatial and temporary fluctuations of the Tonle Sap flow as well as the changes in water level and inundated area of the Tonle Sap; and (2) the hydraulic relation of Tonle Sap with the Mekong River.

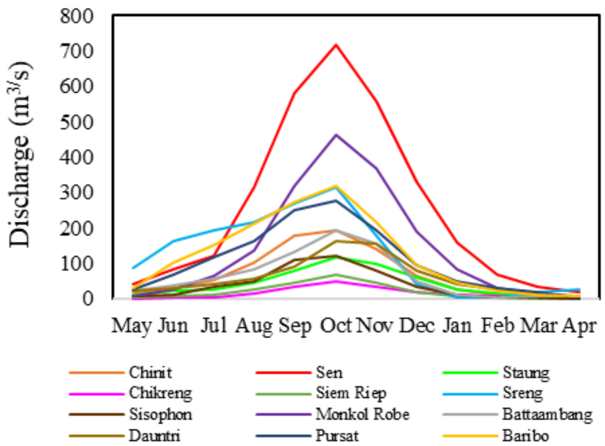

Fig. 13 Average monthly discharge in 12 stations

Results and discussions

Model calibration and verification

Hydrodynamic modeling of a natural domain requires the careful selection of parameters to simulate the physical conditions as closely as possible to real conditions. In addition, the wetting - drying algorithm is also calibrated to maintain numerical stability and a reasonable simulation times.

The calibration period is selected from 1/5/2009 – 30/4/2009 and the verification period is from 1/6/2008 – 30/4/2009 because these periods are representative for average hydrological conditions. The simulated data will be compared with observed water level data in Kompong Luong station (see Fig. 11) that is located in the downstream part of the Tonle Sap lake. The Manning coefficient is used for parameterizing the bottom friction. In this simulation, the optimal Manning coefficient is set to n = 0.035 s/m$^{1/3}$ after referring to previous researches (Hai et al., 2008 and Manh et al., 2014) and applying the trial and error method, and the same value it is applied in the whole domain. The threshold value ε is fixed to be 0.9 m. The quantitative assessment of the model and the algorithm is evaluated by the Nash – Sutcliffe coefficient (NASH), which is used to assess the predictive power of hydrological models as below:

$$NASH = 1 - \frac{\sum_{i=1}^{n}(H_{obs,i} - H_{simu,i})^2}{\sum_{i=1}^{n}(H_{obs,i} - H_{obs})^2} \qquad (8)$$

where H_{obs} is the mean of observed water level, $H_{obs,i}$ is observed water level at time t =i and $H_{simu,i}$ is numerical simulated water level at time t = i, n is number of time steps

In addition, the Root Mean Square Error (RMSE) is also used to evaluate the difference between computed results and observed data.

$$RMSE = \sqrt{\frac{\sum_{i=1}^{n}(H_{obs,i} - H_{simu,i})^2}{n}} \qquad (9)$$

where $H_{simu,i}$ is the numerical simulated result at time t = i and $H_{observed,i}$ is the observed data at the same time and n is the number of time steps.

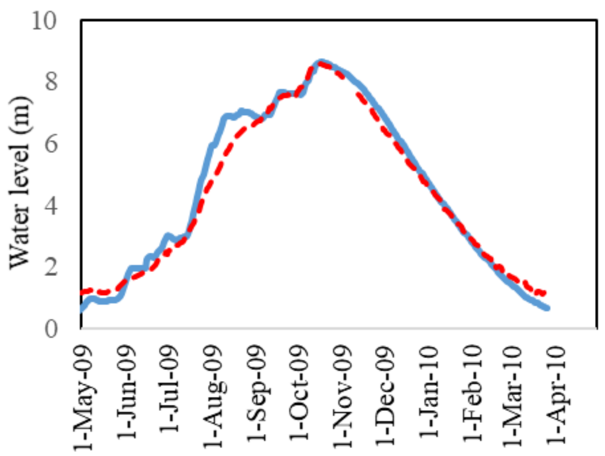

Fig. 14 Calibration of water level in Kompong Luong station from 1/5/2009 to 30/4/2010. The blue continuous line corresponds to the simulated results and the dashed red line corresponds to measured data

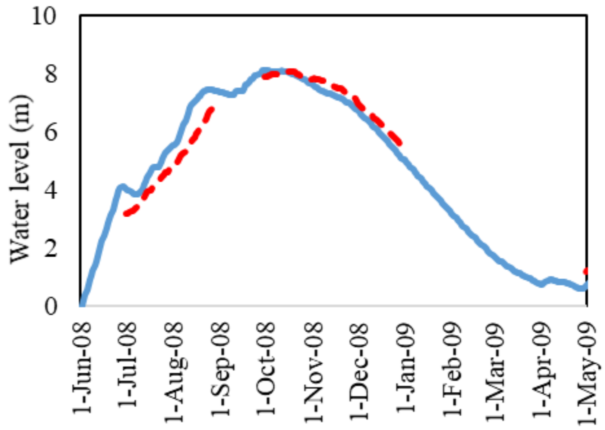

Fig. 15 Verification of water level in Kompong Luong station from 1/6/2008 to 30/4/2009. The blue continuous line shows simulated results and the dashed red line shows measured data

The calibration result of the water level in Kompong Luong station in period of 01/05/2009 – 30/04/2010 shows a very good correlation between measured data and simulated result (see Fig. 14) with NASH coefficient of 98.24 % and RMSE of 1.396 m. The simulated results present good agreement in both amplitude and phase with the measured data. Before simulating for an extremely flooding season in the Lower Mekong Basin, the model verification is conducted over the period of 01/06/2008 – 30/04/2009. The verification results also present a reasonable agreement between modelled and observed data with a NASH coefficient of 88.72 % and RMSE of 2.871 m as seen in Fig. 15. Thus these parameters can be applied for testing different scenarios.

The monthly discharge at Prek Kdam is calculated and compared with the discharge at Kratie, which is located in the Mekong mainstream before dividing into the Tonle Sap and the Mekong Delta; and with the total discharge from 12 tributaries of the Tonle Sap (Fig. 16). The monthly discharge at Prek Kdam shows two groups of values. The negative values mean inflow from the Mekong River towards the lake, that occur during the wet season. The positive values start from November to April, meaning that the flow is outward. The discharge from Kratie and the total discharge from the 12 tributaries show the time lag with maximum value in September and October respectively. As the amplitude of the discharge at Kratie is 10 – 20 times higher than the one of tributaries, it confirms the flow pulse of the Tonle Sap is dominated directly by the flow regime from the Mekong river. This outcome is consistent with studies by Fujii et al. (2003) and Kummu et al. (2014).

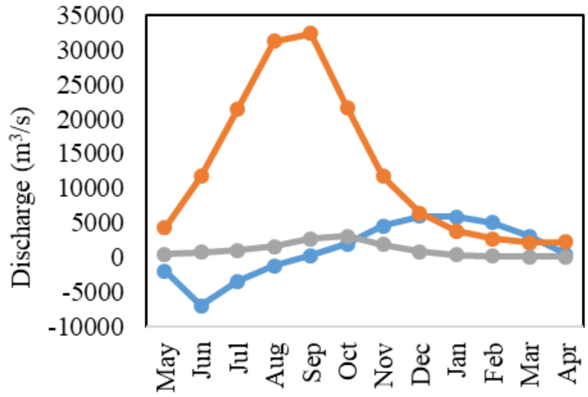

Fig. 16. Monthly discharge at Prek Kdam (blue) and in comparision with discharge at Kratie (orange) and total discharge from 12 tributaries of the Tonle Sap (gray)

Flood seasonal pattern

For further simulation of wetting – drying processes and variations of inundated areas in the Tonle Sap system, a 6-month period of wet season in 2011 hydrological year is selected because this year is regarded as historically extreme in both spatial extent and depth of seasonal inundation across the Cambodia floodplain and the Mekong Delta of Vietnam (MRC, 2015 and see Fig. 17) during 88 years of observation (Manh et al., 2014).

The wetting - drying process can be viewed clearly from the snapshot of water elevation and flow current vectors at different phases during wet season of 2011 flooding year (see Fig. 18). Panels (a) and (b) are representative for the transition period of dry - wet seasons, panels (c), (d),(e), and (f) are for the wet season. The black colour shows wet areas and white colour shows dry areas. The colourful arrows represent for current magnitudes and directions. So, a unique flooding and dewatering pattern is shown, as a result of water level fluctuations with respect to the real topography.

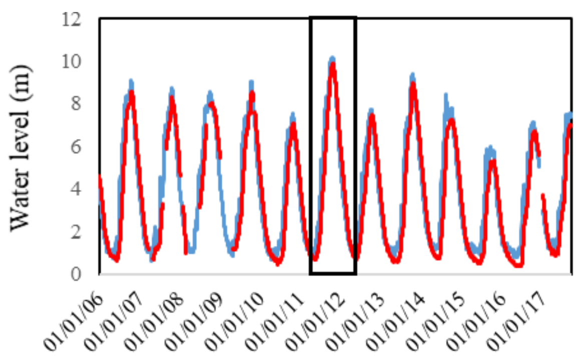

Fig. 17. Water level at Kompong Luong (red line) and Prek Kdam (blue line) from 12 hydrological years 2006 - 2017

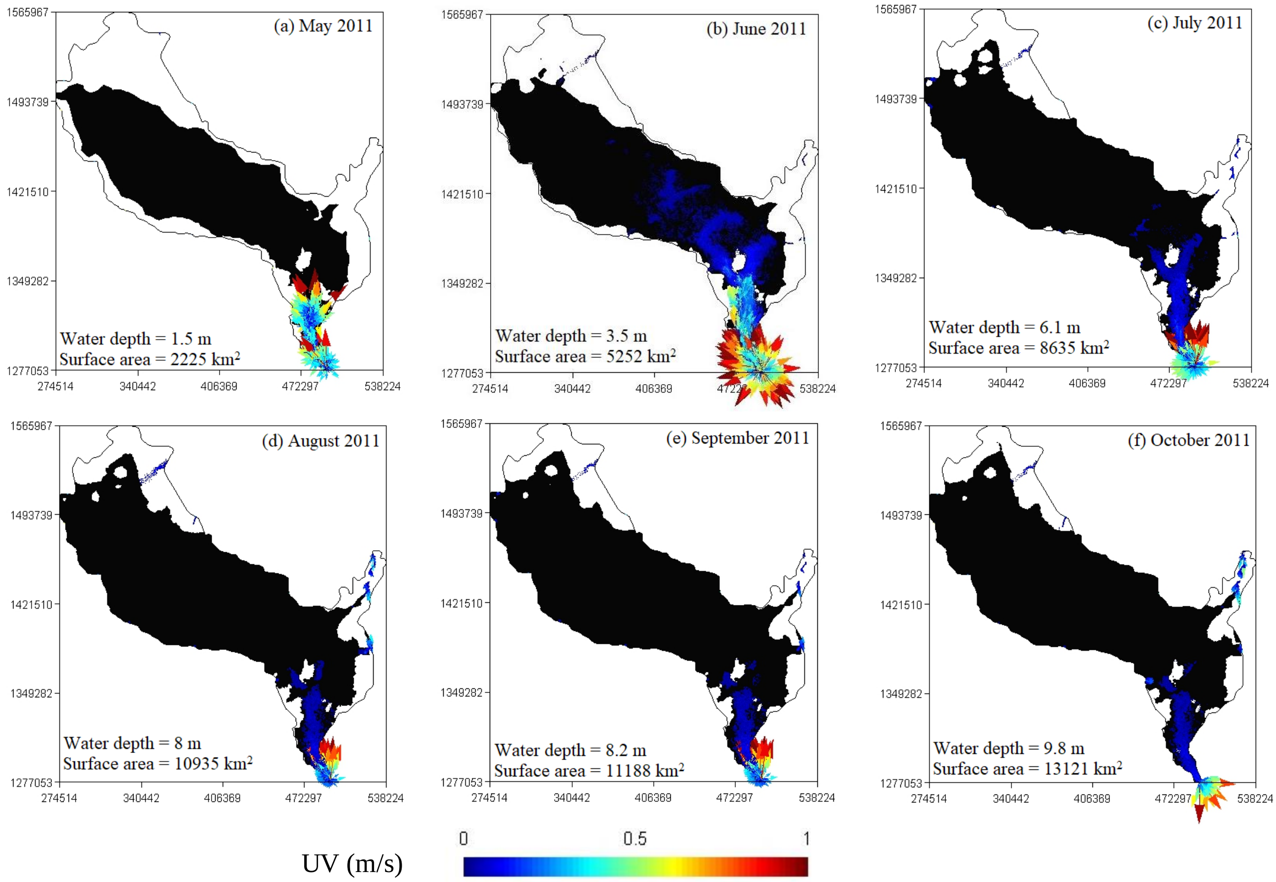

Fig. 18. Surface water area and flow patterns in 6 rainy months of flooding year 2011. The black thin line represents for the boundary of computed domain. The black colour shows inundated areas and white colour shows dry areas. The colour bar describes the flow current magnitudes with scale of 0 – 1 m/s

Fig. 18 (a) represents the results for May 2011. It may be noted that this month is the end of the dry season and the beginning of the flood season, so there are relatively large dry areas, which are located almost over the whole domain. Only the permanent lake is wet with water elevations of 10.5 – 11.5 m, a mean depth of 1.5 m and a wet area of 2225 km^2. The southern part of the domain has the lowest bed elevation, thus the water flows from this point in the northwestern direction to the lake and starts filling up the domain. On the other hand, it takes longer for the slightly higher elevation on the north and northeast to become inundated.

Fig. 18 (b) shows the pattern of June 2011. This month is the beginning of the wet season and the water depth increases sharply to 3.5 m and the wet areas expand on both sides and northern part of the lake. With the current vectors, it is to see the flow in the lake and its tributaries.

In Fig. 18 (c) for July 2011, the water elevation rises up to nearly 6.1 m, with an inundated area of approximately 8635 km^2 and the strongest flow from the Mekong river to the lake. Fig. 18 (d) and Fig. 18 (e) correspond to August and September 2011, which are in the middle of the wet season. Therefore, the water depth is very high with values of approximately 8.0 m. The prevailing flow direction is towards the lake and the dry areas are getting smaller.

October is the end of wet season, as shown in Fig. 18 (f); the water depth reaches its peak at approximately 9.8 m and the maximum inundated area is approximately 13,121 km^2. Approximately 90 % of the floodplain area is covered by water at the peak level. The dry areas are only located in the north, east and mountain of the whole domain. The current is the strongest at Prek Kdam, it is outward of the lake.

Discussion

During the 6 months of wet season, the inundated area has increased by 10,896 km^2 from 2225 km^2 (mean value) to maximum value of 13,121 km^2, corresponding to the variation of water depths between 1.5 m and 9.8 m. This result confirms the close relation between the flood-pulse features of the Tonle Sap Lake originating from flow alterations in the Mekong River. The Tonle Sap flood pulse is controlled by flooding and dewatering phenomena, which are under the direct impact of the flow from the Mekong mainstream (Kummu and Sarkkula, 2008; ADB, 2009 and Ji et al., 2018). This result is similar to those of a study on water balance in

Tonle Sap system conducted by Kummu et al. (2014) and a study on changes on the Tonle Sap lake area performed by Siev et al., (2016) and Ji et al. (2018) using GIS methods.

These results on water level and currents show the ability of the algorithm to well represent wetting and drying processes in a realistic case with complex bathymetry. Water exchanges over the lake – river and floodplain are asymmetric across the Tonle Sap river, and tend to vary periodically on the lake while quickly washing out on the southern part.

CONCLUSIONS

The wetting – drying algorithm successfully implemented in SLIM reproduces well simulations of watering and dewatering processes in both theoretical test cases and in a realistic domain. The method is based on a threshold value and a blending parameter. At each time step, the total water depth in each cell is compared to a user-defined threshold value. If the total water depth is below that value then that cell is considered dry. It shows both local mass conservation and rapid transition of a wet/dry interface.

The simulation results confirm that wetting – drying processes plays an essential role in simulating the flow regime and water depth fluctuations of the Tonle Sap lake as well as the whole system. The simulations results also reveal the spatial and temporary distribution of the surface water areas and currents in the floodplain, which are controlled by imposed discharge from 12 tributaries as well as water level in the downstream boundary at Prek Kdam. Seasonal variations in the inundated area of the Tonle Sap lake were dominantly influenced by runoff from the Mekong River. The modelled results can also regenerate discharge and water level at locations, where are lack of monitoring hydrological data.

ACKNOWLEDGEMENTS

The PhD fellowship of Hoang-Anh Le is provided by the Université catholique de Louvain, Belgium. The research has been conducted under the framework of CARE-Rescif initiative with grant number Tc-TTC-2017-08. Computational resources have been provided by the Consortium des Équipements de Calcul Intensif (CÉCI), funded by the Fonds de la Recherche Scientifique de Belgique (F.R.S.-FNRS) under Grant No.2.5020.11.

REFERENCES

Asian Development Bank - ADB (2009). Cambodia: Preparing the Water Resources Management (Sector) Project. Water Resources Management Sector Development Project Technical Annex on Integrated Water Resources Management (IWRM). Phnom Penh: Ministry of Water Resources and Meteorology, Royal Government of Cambodia and Asian Development Bank.

Balzano, A. (1998). Evaluation of methods for numerical simulation of wetting and drying in shallow water flow models. Coastal Engineering, 34(1-2), 83-107.

Berg, M., Stengel, C., Trang, P. T. K., Viet, P. H., Sampson, M. L., Leng, M., ... & Fredericks, D. (2007). Magnitude of arsenic pollution in the Mekong and Red River Deltas—Cambodia and Vietnam. Science of the Total Environment, 372(2-3), 413-425.

Campbell, I. C., Say, S., and Beardall, J. (2009). Tonle Sap Lake, the heart of the lower Mekong. In The Mekong (pp. 251-272).

Casulli, V. (2009). A high-resolution wetting and drying algorithm for free - surface hydrodynamics. International Journal for Numerical Methods in Fluids, 60(4), 391-408.

D'Alpaos, L., & Defina, A. (2007). Mathematical modeling of tidal hydrodynamics in shallow lagoons: A review of open issues and applications to the Venice lagoon. Computers & Geosciences, 33(4), 476-496.

De Brye, B., de Brauwere, A., Gourgue, O., Kärnä, T., Lambrechts, J., Comblen, R., & Deleersnijder, E. (2010). A finite-element, multi-scale model of the Scheldt tributaries, river, estuary and ROFI. Coastal Engineering, 57(9), 850-863.

De Brye, B., Schellen, S., Sassi, M., Vermeulen, B., Kärnä, T., Deleersnijder, E., & Hoitink, T. (2011). Preliminary results of a finite-element, multi-scale model of the Mahakam Delta (Indonesia). Ocean Dynamics, 61(8), 1107-1120.

Dresback, K. M., Kolar, R. L., & Dietrich, J. C. (2002). Impact of the form of the momentum equation on shallow water models based on the generalized wave continuity equation. Development in Water science, 47, 1573-1580.

Fujii, H., Garsdal, H., Ward, P., Ishii, M., Morishita, K., & Boivin, T. (2003). Hydrological roles of the Cambodian floodplain of the Mekong River. International Journal of River Basin Management, 1(3), 253-266.

Geuzaine, C., and Remacle, J. F. (2009). Gmsh: A 3-D finite element mesh generator with built-in pre-and post-processing facilities. International journal for numerical methods in engineering, 79(11), 1309-1331.

Gourgue, O., Deleersnijder, E., & White, L. (2007). Toward a generic method for studying water renewal, with application to the epilimnion of Lake Tanganyika. Estuarine, Coastal and Shelf Science, 74(4), 628-640.

Gourgue, O., Comblen, R., Lambrechts, J., Kärnä, T., Legat, V., & Deleersnijder, E. (2009). A flux-limiting wetting–drying method for finite-element shallow-water models, with application to the Scheldt Estuary. Advances in Water Resources, 32(12), 1726-1739.

Gourgue, O., Baeyens, W., Chen, M. S., de Brauwere, A., de Brye, B., Deleersnijder, E., ... & Legat, V. (2013). A depth-averaged two-dimensional sediment transport model for environmental studies in the Scheldt Estuary and tidal river network. Journal of Marine Systems, 128, 27-39.

Hai, P. T., Masumoto, T., and Shimizu, K. (2008). Development of a two-dimensional finite element model for inundation processes in the Tonle Sap and its environs. Hydrological processes, 22(9), 1329-1336.

Heniche, M., Secretan, Y., Boudreau, P., & Leclerc, M. (2000). A two-dimensional finite element drying-wetting shallow water model for rivers and estuaries. Advances in Water Resources, 23(4), 359-372.

Ji, X., Li, Y., Luo, X., He,. D. (2018) Changes in the Lake Area of Tonle Sap: Possible Linkage to Runoff Alterations in the Lancang River? Remote Sensing, 10(6), 866-886.

Kärnä, T., De Brye, B., Gourgue, O., Lambrechts, J., Comblen, R., Legat, V., & Deleersnijder, E. (2011). A fully implicit wetting–drying method for DG-FEM shallow water models, with an application to the Scheldt Estuary. Computer Methods in Applied Mechanics and Engineering, 200(5-8), 509-524.

Kesserwani, G., & Liang, Q. (2012). Dynamically adaptive grid based discontinuous Galerkin shallow water model. Advances in water resources, 37, 23-39.

Kummu, M., & Sarkkula, J. (2008). Impact of the Mekong River flow alteration on the Tonle Sap flood pulse. AMBIO: A Journal of the Human Environment, 37(3), 185-192.

Kummu, M., Tes, S., Yin, S., Adamson, P., Józsa, J., Koponen, J., ... and Sarkkula, J. (2014). Water balance analysis for the Tonle Sap Lake–floodplain system. Hydrological Processes, 28(4), 1722-1733.

Lambrechts, J., Comblen, R., Legat, V., Geuzaine, C., & Remacle, J. F. (2008). Multiscale mesh generation on the sphere. Ocean Dynamics, 58(5-6), 461-473.

Lambrechts, J., Humphrey, C., McKinna, L., Gourge, O., Fabricius, K. E., Mehta, A. J., ... & Wolanski, E. (2010). Importance of wave-induced bed liquefaction in the fine sediment budget of Cleveland Bay, Great Barrier Reef. Estuarine, Coastal and Shelf Science, 89(2), 154-162.

Manh, N. V., Dung, N. V., Hung, N. N., Merz, B., & Apel, H. (2014). Large-scale suspended sediment transport and sediment deposition in the Mekong Delta. Hydrology and Earth System Sciences, 18(8), 3033.

Marras, S., Kopera, M. A., Constantinescu, E. M., Suckale, J., & Giraldo, F. X. (2016). A continuous/discontinuous Galerkin solution of the shallow water equations with dynamic viscosity, high-order wetting and drying, and implicit time integration. arXiv preprint arXiv:1607.04547.

Martins, R., Leandro, J., & Djordjević, S. (2018). Wetting and drying numerical treatments for the Roe Riemann scheme. Journal of Hydraulic Research, 56(2), 256-267.

Medeiros, S. C., & Hagen, S. C. (2013). Review of wetting and drying algorithms for numerical tidal flow models. International journal for numerical methods in fluids, 71(4), 473-487.

MRC (2015) Annual Mekong Flood Report 2011, Mekong River Commission, 72 pages.

Nielsen, C., & Apelt, C. (2003). Parameters affecting the performance of wetting and drying in a two-dimensional finite element long wave hydrodynamic model. Journal of Hydraulic Engineering, 129(8), 628-636.

Penny, D. (2006). The Holocene history and development of the Tonle Sap, Cambodia. Quaternary Science Reviews, 25(3-4), 310-322.

Pham Van Chien (2014). Development of a finite element model simulating flow and sediment dynamics: Application to the Mahakam land-sea continuum (Indonesia). Ph.D. Thesis. Université Catholique de Louvain, Belgium

Pham Van Chien., de Brye, B., Deleersnijder, E., Hoitink, A. J. F., Sassi, M., Spinewine, B., ... & Soares-Frazão, S. (2016). Simulations of the flow in the Mahakam river–lake–delta system, Indonesia. Environmental Fluid Mechanics, 16(3), 603-633.

RoyalHaskoningHDV, Deltares, UNESCO-IHE, 2010. The flood management and mitigation programme. Component 2: Structural measures and flood proofing in the Lower Mekong Basin.

Smagorinsky, J. (1963). General circulation experiments with the primitive equations: I. The basic experiment. Monthly weather review, 91(3), 99-164.

Siev, S., Paringit, E. C., Yoshimura, C., and Hul, S. (2016). Seasonal Changes in the Inundation Area and Water Volume of the Tonle Sap River and Its Floodplain. Hydrology, 3(4), 33.

Thacker, W. C. (1981). Some exact solutions to the nonlinear shallow-water wave equations. Journal of Fluid Mechanics, 107, 499-508.

Thanh, V. Q., Reyns, J., Wackerman, C., Eidam, E. F., and Roelvink, D. (2017). In press. Modelling suspended sediment dynamics on the subaqueous delta of the Mekong River. Continental Shelf Research.

Vallaeys, V., Kärnä, T., Delandmeter, P., Lambrechts, J., Baptista, A. M., Deleersnijder, E., & Hanert, E. (2018). Discontinuous Galerkin modeling of the Columbia River's coupled estuary-plume dynamics. Ocean Modelling.

Vater, S., Beisiegel, N., & Behrens, J. (2015). A limiter-based well-balanced discontinuous Galerkin method for shallow-water flows with wetting and drying: One-dimensional case. Advances in water resources, 85, 1-13.

Vincent, D., Karatekin, Ö., Vallaeys, V., Hayes, A. G., Mastrogiuseppe, M., Notarnicola, C., ... & Deleersnijder, E. (2016). Numerical study of tides in Ontario Lacus, a hydrocarbon lake on the surface of the Saturnian moon Titan. Ocean Dynamics, 66(4), 461-482.

Warner, J. C., Defne, Z., Haas, K., & Arango, H. G. (2013). A wetting and drying scheme for ROMS. Computers & geosciences, 58, 54-61.

Yuan, D., Lin, B., & Falconer, R. (2008). Simulating moving boundary using a linked groundwater and surface water flow model. Journal of hydrology, 349(3-4), 524-535.

Zheng, L., Chen, C., & Liu, H. (2003). A modeling study of the Satilla River Estuary, Georgia. I: Flooding-drying process and water exchange over the salt marsh-estuary-shelf complex. Estuaries, 26(3), 651-669.